Supporting Information

Self-Assembly of Mixtures of Telechelic and Monofunctional Amphiphilic Polymers in Water: From Clusters to Flowerlike Micelles

Thomas Zinn, Lutz Willner, Kenneth D. Knudsen, and Reidar Lund

Materials

Fractionation of difunctional PEO

The crude material of the coupling reaction was fractionated with chloroform/heptane as solvent/non-solvent pair for PEO. To monitor the effect of the fractionation, SEC chromatograms were taken from each fraction. Elution curves of six fractions of $C_{22}-PEO10-C_{22}/$ $C_{22}-PEO5$ are exemplary shown in Figure S1 together with the SEC curve of the crude product. Fractions 1 and 2 show significant enrichment of a chain-extended by-product arising from the coupling reaction of a modicum of residual α,ω-dihydroxy-PEO10 with n-alkyl-PEO5. Both fractions were discarded. Fractions 3 - 6 are essentially free of the high molecular weight by-products. Compared to the crude polymer the triblock/diblock ratio is larger but becomes smaller for higher fractions. Simultaneously, the chromatograms reveal a slight shift of the peak position indicating a small change on molar mass due to fractionation. The fractions 3 - 6 were combined, chloroform was evaporated and the residual polymer freeze-dried from benzene. The yield was 75 % with respect to the crude polymer.
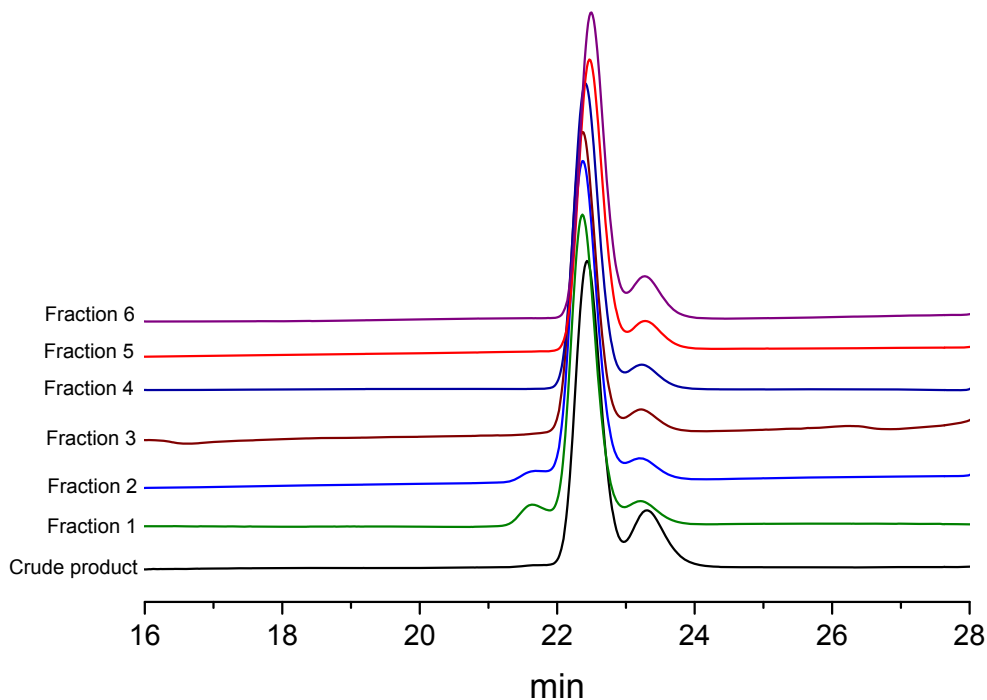
Figure S1: SEC-curves of crude product and different fractions of $C_{22}-PEO10-C_{22}/C_{22}-PEO5$.

NMR Characterization

The number average molecular weight of the final product was determined by ^{1}H-NMR measurements in deuterochloroform. Spectra were recorded with a Bruker Avance III 600 MHz sprectrometer equipped with CryoProbe Prodigy. The spectrum of $C_{22}-PEO10-C_{22}$ is depicted in Figure S2. For comparison also the spectrum of the pure diblock is shown. The two spectra are essentially identical except for the signal at 3.73 ppm which stems from the methylene protons adjacent to the terminal hydroxy group of the PEO in the diblock. The signal almost disappears in the coupling product due to the formation of the ether linkage. M_n (PEO) was calculated taking the signals of the n-alkyl group as internal reference. M_n (PEO) of the triblock/diblock mixture differs slightly from twice the M_n of the precursor diblock because of the fractionation with chloroform/heptane.
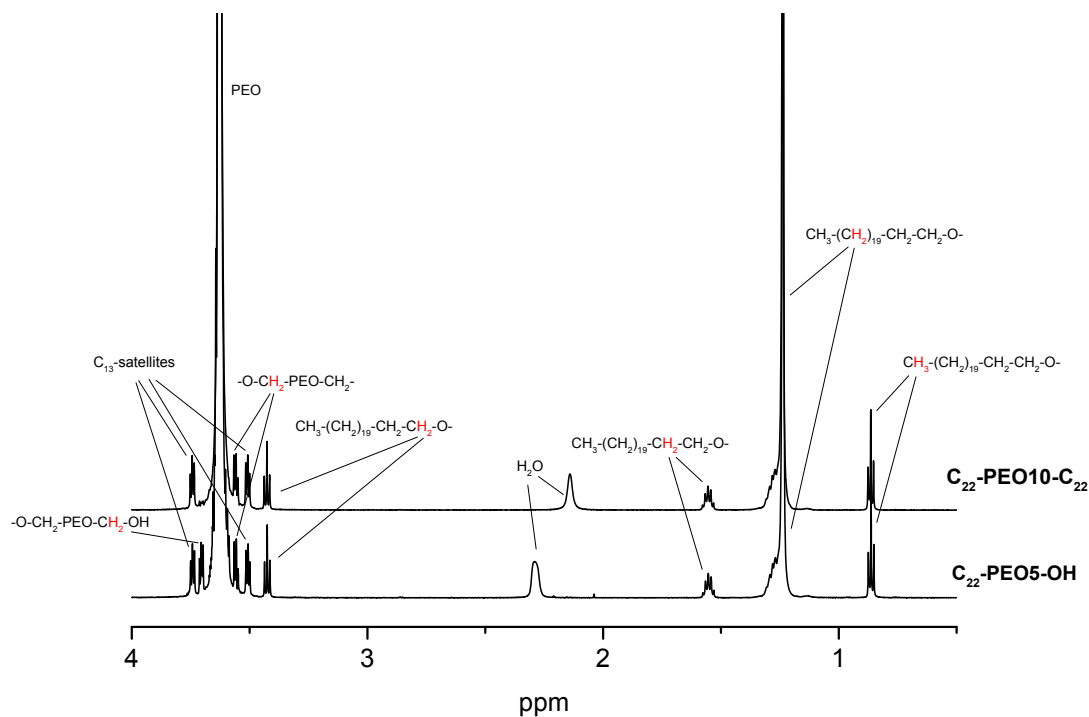
Figure S2: ^{1}H-NMR spectra of $C_{22}-PEO5$ and $C_{22}-PEO10-C_{22}/C_{22}-PEO5$ Integrals $C_{22}-PEO10-C_{22}$: PEO: 452; $-O-CH_2-PEO-CH_2$: 2.01; $CH_3-(CH_2)_{18}-CH_2-CH_2-O-$: 2.09: $CH_3-(CH_2)_{18}-CH_2-CH_2-O-$: 2.02; $CH_3-(CH_2)_{18}-CH_2-CH_2-O-$: 38; $CH_3-(CH_2)_{18}-CH_2-CH_2-O-$: 3. Integrals $C_{22}-PEO5$: PEO: 445; $-O-CH_2-PEO-CH_2$: 2.07; $CH_3-(CH_2)_{18}-CH_2-CH_2-O-$: 2.1: $CH_3-(CH_2)_{18}-CH_2-CH_2-O-$: 1.95; $CH_3-(CH_2)_{18}-CH_2-CH_2-O-$: 38; $CH_3-(CH_2)_{18}-CH_2-CH_2-O-$: 3.06; $-O-CH_2-PEO-CH_2-OH$: 2.07.

3

Small-angle neutron scattering (SANS)

Data Treatment

The small-angle neutron scattering experiments were carried out at the SANS installation at the JEEP-II reactor at Kjeller, Norway. The instrument is equipped with a liquid hydrogen moderator, which shifts the D_2O moderated thermal neutron spectrum (intensity maximum at approximately $1\,\text{Å}$) toward longer wavelengths. A silicon-wafer based bender is installed in the beam path to deflect cold neutrons (cutoff at $4.5\,\text{Å}$), and reduce gamma radiation and thermal/fast neutrons. The wavelength was set with a velocity selector (Dornier), using a wavelength resolution ($\Delta\lambda/\lambda$) of 10%. The beam divergence was set by an input collimator (18.4 or $8.0\,\text{mm}$ diameter) located $2.3\,\text{m}$ from the sample, together with a circular $7\,\text{m}$ aperture located close to the sample that defined the beam cross section. A $1.8\,\text{m}$ long evacuated flight tube separates the collimators. The detector was a 128 128 pixel, $59\,\text{cm}$ active diameter, ^3He-filled RISØ type detector, mounted on rails inside the evacuated detector chamber. The sample-detector distance was varied between 1.0 and $3.4\,\text{m}$, using the wavelengths 5.1 and $10.2\,\text{Å}$, respectively. Each complete scattering curve was composed of three independent measurements, using different wavelength-distance combinations ($5.1\,\text{Å}/1.0\,\text{m}$, $5.1\,\text{Å}/3.4\,\text{m}$, and $10.2\,\text{Å}/1.0\,\text{m}$). The resulting Q-range for the experiment was 0.006 - 0.3 Å^{-1}. The solutions were filled in 2 mm Starna quartz cuvettes. The cells were placed onto a copper-base for good thermal contact and mounted onto the sample stage in the sample chamber. The temperature of the samples was controlled by a water circulator, maintaining the temperature set value to within $\pm 0.1\,°\text{C}$. In all of the SANS measurements, deuterium oxide was used as a solvent instead of H_2O to obtain good contrast and low background for the neutron-scattering experiments. Standard reductions of the scattering data, including transmission corrections, were conducted by incorporating data collected from the empty

cell, and the blocked-beam background, according to the formula given in Eq. (S1).

$$I_{\mathrm{S}}^{\mathrm{corr}} = \left(\frac{I_{\mathrm{S}}}{M_{\mathrm{S}}} - \frac{I_{\mathrm{BG}}}{M_{\mathrm{BG}}} \right) - \frac{T}{T_{\mathrm{EC}}} \left(\frac{I_{\mathrm{EC}}}{M_{\mathrm{EC}}} - \frac{I_{\mathrm{BG}}}{M_{\mathrm{BG}}} \right) \tag{S1}$$

Here I_{S} is the measured scattered intensity for the sample inside the quartz cell, I_{BG} is the intensity of blocked-beam background, and I_{EC} is the intensity of empty quartz cell. T_{S} and T_{EC} are the transmission values (< 1) of the sample and of the empty cell, respectively. The latter are measured by registering the intensity of the direct beam spot with the beam stop moved aside and with an attenuator in the beam to avoid saturation of the detector. All the measurements were normalized to the beam monitor counts (M_i) to compensate for any possible variations in the incoming beam flux. The data correction shown in Eq. (S1) is done in each pixel of the detector matrix. Finally, all data were transformed to an absolute scale (coherent differential macroscopic cross section $\mathrm{d}\Sigma/\mathrm{d}\Omega$), making use of the intensity value registered in open beam measurements (no sample or cell), with a calibrated attenuator (Cd-mask with holes) in the beam,[1] before averaging radially to produce an $\mathrm{d}\Sigma/\mathrm{d}\Omega$ vs. Q scattering profile where $Q = 4\pi\lambda^{-1}\sin(\vartheta/2)$.

Modified Baxter structure factor model

The basic result of the model by Menon $et\ al.$[2] is a perturbative first-order solution of the Ornstein-Zernike equation and the Percus-Yevick closure relation.[3] The expression of the structure factor $S_{\mathrm{app}}(Q)$ is given by

$$
\begin{aligned}
S_{\mathrm{app}}(Q) &= \frac{1}{A(Q)^2 + B(Q)^2} \tag{S2}\\
A(Q) &= 1 + 12\,\eta \left[\alpha\,\frac{\sin\kappa - \kappa\cos\kappa}{\kappa^3} + \beta\frac{1-\cos\kappa}{\kappa^2} - \frac{\lambda}{12}\frac{\sin\kappa}{\kappa} \right] \tag{S3}\\
B(Q) &= 12\,\eta \left[\alpha\left(\frac{1}{2\kappa} - \frac{\sin\kappa}{\kappa^2} + \frac{1-\cos\kappa}{\kappa^3} \right) + \beta\left(\frac{1}{\kappa} - \frac{\sin\kappa}{\kappa^2} \right) - \frac{\lambda}{12}\frac{1-\cos\kappa}{\kappa} \right] \tag{S4}
\end{aligned}
$$

where the internal model parameters are defined as

$$\alpha = \frac{1+2\eta-\mu}{(1-\eta)^2} \qquad \beta = \frac{\mu-3\eta}{2\,(1-\eta)^2} \qquad \mu = \lambda\eta(1-\eta) \tag{S5}$$

$$\lambda\tau = \frac{1+\eta/2}{(1-\eta)^2} + \lambda\left(\frac{\eta}{12} - \frac{\eta^2}{1-\eta}\right) \qquad \kappa = Q\,(2\,R_{\mathrm{HS}} + \Delta) \tag{S6}$$

here λ is an unknown parameter as introduced by Baxter.[4] The parameter $\eta = \pi\,\varrho_n\,(2\,R_{\mathrm{HS}} + \Delta)^3/6$ is the effective particle volume fraction with the number density ϱ_n of the dispersed particles and τ is a measure of the attractive strength which is related to the potential parameters $(u_0, \Delta, R_{\mathrm{HS}})$ and the temperature T

$$\tau = \frac{2\,R_{\mathrm{HS}} + \Delta}{12\,\Delta}\,\exp(u_0/k_B T) \tag{S7}$$

with k_B as Boltzmann constant.

Compensation for deviations from the dilute limit

The Percus-Yevick[3] structure factor $S_{\mathrm{PY}}(Q)$ is used to account for slight deviations from the dilute limit. This was necessary only for the micelles formed by the monofunctionalized PEO polymers and only in the case of n=16 and 22. Since the additional inter-micellar interferences are convoluted with the scattering data we simple multiplied $S_{\mathrm{PY}}(Q)$ according to

$$\frac{d\Sigma}{d\Omega}(Q) = \frac{\phi}{V_{\mathrm{mic}}}\,P_{\mathrm{mic}}(Q)\,S_{\mathrm{PY}}(Q) \tag{S8}$$

All other data was modeled as given in the theoretical section of the main manuscript.

References

(1) Wignall, G. D.; Bates, F. S. Absolute calibration of small-angle neutron scattering data. *J. Appl. Crystallogr.* **1987**, *20*, 28.

(2) Menon, S. V. G.; Manohar, C.; Rao, K. S. A new interpretation of the sticky hard sphere model. *J. Chem. Phys.* **1991**, *95*, 9186.

(3) Wertheim, M. Exact Solution of the Percus-Yevick Integral Equation for Hard Spheres. *Phys. Rev. Lett.* **1963**, *10*, 321.

(4) Baxter, R. J. Percus–Yevick equation for hard spheres with surface adhesion. *J. Chem. Phys.* **1968**, *49*, 2770.